Future Integrative Medicine **2024** vol. 3(4) | 222–238
DOI: 10.14218/FIM.2024.00037

Original Article

Identification of Chemical Constituents and Blood-absorbed Components of Shenqi Fuzheng Extract Based on UPLC-Triple-TOF/MS Technology

Menglei Wang[1,2#], Bingjie Zhu[1,2#], Meng Gao[1,2], Yining Hu[1,2], Xiang Li[1,3], Liangfeng Liu[4], Zhiwei Ge[5], Wenhua Huang[4], Jie Liao[1,2*] and Xiaohui Fan[1,2,6*]

[1]College of Pharmaceutical Sciences, Zhejiang University, Hangzhou, Zhejiang, China; [2]Future Health Laboratory, Innovation Center of Yangtze River Delta, Zhejiang University, Jiaxing, Zhejiang, China; [3]School of Basic Medical Sciences and Forensic Medicine, Hangzhou Medical College, Hangzhou, Zhejiang, China; [4]Limin Pharmaceutical Factory, Livzon Pharmaceutical Group Inc., Shaoguan, Guangdong, China; [5]Analysis Center of Agrobiology and Environmental Sciences, Zhejiang University, Hangzhou, China; [6]The Joint-laboratory of clinical multi-omics research between Zhejiang University and Ningbo Municipal Hospital of TCM, Ningbo Municipal Hospital of TCM, Ningbo, Zhejiang, China

Received: August 04, 2024 | **Revised:** October 26, 2024 | **Accepted:** October 29, 2024 | **Published online:** December 04, 2024

Abstract

Background and objectives: Shenqi Fuzheng (SQ) is a widely used Chinese medicine formula known for its immune-enhancing and Qi-supplementing properties. However, the blood-absorbed components of SQ and their pharmacokinetics remain underexplored. This study aimed to comprehensively analyze the chemical constituents of SQ and investigate their absorption and pharmacokinetic behavior in rat plasma.

Methods: Ultra-performance liquid chromatography-triple quadrupole time-of-flight mass spectrometry (hereinafter referred to as UPLC-Triple-TOF/MS) is employed to identify the chemical components in SQ extract and quantify the components absorbed into the blood after oral administration in rats. This method provides fragmentation patterns of compounds and key pharmacokinetic profiles of blood-absorbed compounds.

Results: A total of 105 compounds are identified from the SQ extract, and 40 are detected in the blood following oral administration. Organic acids and amino acids are found at higher concentrations in the bloodstream. Compounds such as Astragalosides promptly enter the bloodstream within 5 m after administration, with levels declining after 15 m. Flavonoids are absorbed within 15–30 m, and the peak of alkaloids occurs approximately 1 h after administration.

Conclusions: This study provides new insights into the chemical composition and pharmacokinetics of SQ, highlighting the dynamic changes in the content of absorbed compounds in the blood. It further promotes the comprehensive characterization of traditional Chinese medicine formulations through UPLC-Triple-TOF/MS. Future research should focus on elucidating the pharmacological activities of the identified compounds and investigating their potential synergistic effects within the formulation.

Keywords: Traditional Chinese medicine; Ultra-performance liquid chromatography-triple quadrupole time-of-flight mass spectrometry; UPLC-Triple-TOF/MS; Chemical composition; Blood-absorbed components; Chinese medicine compound; Shenqi Fuzheng.

***Correspondence to:** Jie Liao and Xiaohui Fan, College of Pharmaceutical Sciences, Zhejiang University, Hangzhou 310058, Zhejiang, China. ORCID: https://orcid.org/0000-0002-6697-8998 (JL); https://orcid.org/0000-0002-6336-3007 (XHF). Tel: +86-18768118297 (JL); +86-571-88208596 (XHF), E-mail: liaojie@zju.edu.cn (JL); fanxh@zju.edu.cn (XHF)

[#]These authors contributed equally to this work.

How to cite this article: Wang M, Zhu B, Gao M, Hu Y, Li X, Liu L, *et al*. Identification of Chemical Constituents and Blood-absorbed Components of Shenqi Fuzheng Extract Based on UPLC-Triple-TOF/MS Technology. *Future Integr Med* 2024;3(4):222–238. doi: 10.14218/FIM.2024.00037.

Introduction

Traditional Chinese medicine (TCM), particularly Chinese medicine compounds, plays a central role in treating various diseases.[1–3] Shenqi Fuzheng (SQ) formula and its derived preparations are prominent examples that have been extensively utilized in modern medical practices.[4–6] SQ is composed of two traditional Chinese medicinal herbs: *Radix Codonopsis pilosula* (known as Dangshen in Chinese, from *Codonopsis pilosula (Franch.) Nannf.*) and *Radix Astragali* (known as Huangqi in Chinese, from *Astragalus membranaceus (Fisch.) Bunge*).[7] Both herbs are traditionally used to

supplement Qi (according to TCM theory).[8,9] Clinically, SQ has been applied for purposes ranging from enhancing immune function to cancer treatment.[10–12]

As a TCM prescription, the SQ formula contains complex components and a variety of bioactive compounds that exert therapeutic effects.[8,13] This complexity presents significant challenges in identifying and characterizing individual components. Mass spectrometry (MS), combined with advanced separation techniques, has become a key tool for revealing the complex chemical components of TCM formulations.[14] Techniques such as ultra-performance liquid chromatography-triple quadrupole time-of-flight MS (UPLC-Triple-TOF/MS) provide high sensitivity and accuracy, allowing for the structural resolution and detection of a wide range of metabolites, proteins, and other bioactive molecules in complex herbal mixtures.[15–18]

In recent years, significant progress has been made in identifying the chemical constituents of *Radix Astragali* and *Radix Codonopsis*. Jia *et al*.[19] employed UPLC-Triple-TOF/MS to identify 29 compounds in *Radix Codonopsis*, including three alkaloids, 13 phenolic acids, eight alcohol glycosides, and five alkynosides. Liang *et al*.[20] used UPLC-Q-TOF-MS to identify a total of 45 chemical constituents in *Radix Astragali*, including 22 flavonoids, 13 saponins, and 10 amino acids. Furthermore, mass spectrometric analysis has provided insights into the major fragmentation patterns of compounds in the SQ formula. For flavonoids, one of the key groups of bioactive components, major mass spectrometric fragmentation patterns include cleavage of glycosidic bonds, retro-Diels–Alder cleavage, and the loss of neutral fragments such as CO, H_2O, and C_2H_2O.[20] For saponins, most of the MS^2 fragmentation patterns involve the cleavage of glycosidic bonds, with one or more H_2O molecules potentially lost during the fragmentation process. Understanding these major mass spectrometric fragmentation patterns will facilitate compound identification in subsequent studies.

Despite extensive studies on individual components of *Radix Astragali* and *Radix Codonopsis*, studies specifically targeting the chemical components of SQ formula are still limited. Additionally, most bioactive constituents in TCM exhibit pharmacological effects only after being absorbed into the bloodstream,[21] and the specific components of SQ that can enter the blood, along with their pharmacokinetic properties, remain poorly understood. Therefore, further studies on the bioactive components of the formulation and their pharmacokinetics are needed.

In this article, UPLC-Triple-TOF/MS is used to analyze the chemical constituents of the SQ extract and the plasma components of rats post-oral administration. Furthermore, the fragmentation patterns of chemical components and the pharmacokinetic characteristics of the blood compounds are investigated. This will facilitate pharmacological studies of these TCM compounds.

Materials and methods

Drug sample preparation

SQ is prepared by extracting *Radix Codonopsis pilosula and Radix Astragali* at a ratio of 1:1. The extraction process involves separately processing *Radix Codonopsis pilosula* and *Radix Astragali*. These extracts are distilled into concentrates and then treated with ethanol. The resulting concentrates are mixed to produce the SQ extract.[8] SQ extract (2.28 g/mL crude drug, lot number: 231201) is provided by Limin Pharmaceutical Factory, Livzon Pharmaceutical Group. The extract is centrifuged at 10,000 rpm for 10 m, and the resulting supernatant is used as the standard solution.

The reference standards are purchased from Shanghai Winherb Medical Technology Co., Ltd. These standards include Caffeic acid (lot number: 240324), Astragaloside I (lot number: 240410), Isoastraloside I (lot number: 240330), Astragaloside II (lot number: 240415), Isoastraloside II (lot number: 240328), Astragaloside III (lot number: 231207), Calycosin (lot number: 240322), Astragaloside IV (lot number: 240120), Calycosin-7-O-β-D-glucoside (lot number: 231218), and Lobetyolin (lot number: 231206). These standards are dissolved in methanol to prepare 1 mg/mL stock solutions, which are then combined to create a mixed standard solution for analysis. This mixed standard solution is also centrifuged at 10,000 rpm for 10 m, and the supernatant is used for subsequent analyses.

Animal plasma sample preparation

Male Sprague Dawley rats (220 g) are purchased from Shanghai SLAC Laboratory Animal Co., Ltd. (Shanghai, China). The rats are housed under a 12-h light/dark cycle in a controlled environment with food and water provided ad libitum.

The rats are divided into two groups: the control group receives a gavage of 1.6 mL of 0.9% NaCl solution, while the drug group is gavaged with 1.6 mL of SQ extract. Blood samples are collected from the inferior vena cava at 5, 15, 30 m, and 1 h post-gavage into ethylene diamine tetraacetic acid (EDTA)-coated anticoagulant tubes. After allowing the blood to stand for 30 m, the samples are centrifuged at 3,000 rpm to separate the plasma. For plasma preparation, 100 μL of plasma is transferred into a centrifuge tube, mixed with 300 μL of methanol, and thoroughly vortexed for 2 m. The mixture is left in an ice bath for 10 m, followed by centrifugation at 10,000 rpm for 10 m. The resulting supernatant is used as the plasma test solution.

Chromatographic experiments and mass spectrometry

Chromatographic separation is achieved using a Waters ACQUITY UPLC HSS T3 column (1.8 μm particle size, 150 × 2.1 mm). Data acquisition is performed on an Acquity™ UPLC system (Waters Technologies, U.S.A.) coupled to a UPLC-Triple-TOF/MS system (6600+ QTof, SCIEX, Waters Technologies, U.S.A.). The mobile phase A is water with 0.1% formic acid, and the mobile phase B is acetonitrile with 0.1% formic acid. The gradient elution conditions are as follows: 0.00–6.00 m, 2% B; 6.00–20.00 m, 15% B; 20.00–30.00 m, 50% B; 30.00–32.00 m, 95% B. The flow rate is 0.300 mL/m, the column temperature is 50°C, and the injection volume is 3 μL.

Accurate mass measurement is conducted in both negative ion mode and positive ion mode under the following conditions: scan range: mass-to-charge ratio (m/z) 100–2,000 Da and 50–1,500 Da; gas 1 pressure: 55 psi; gas 2 pressure: 55 psi; curtain gas: 35 psi; ion source temperature: 550°C (positive) and 550°C (negative); ion source voltage: 5,500 V (positive) and −4,500 V (negative); first scan: declustering potential: 80 V; collision energy: 10 V; second scan: TOF MS-Product Ion-information-dependent acquisition mode for mass spectrometry data acquisition, with Collision-induced dissociation energy of 40 ± 20 eV. Before injection, a calibrant delivery system pump is used for mass axis calibration to ensure a mass axis error of less than 2 ppm.

Analysis of chemical constituents of SQ extract

For pre-processing, raw mass data of the SQ extract and plasma samples are imported into MS-DIAL software (version 4.9). Peak detection parameters are set with a minimum peak height of 10,000, while all other settings remain at default. Peak alignment

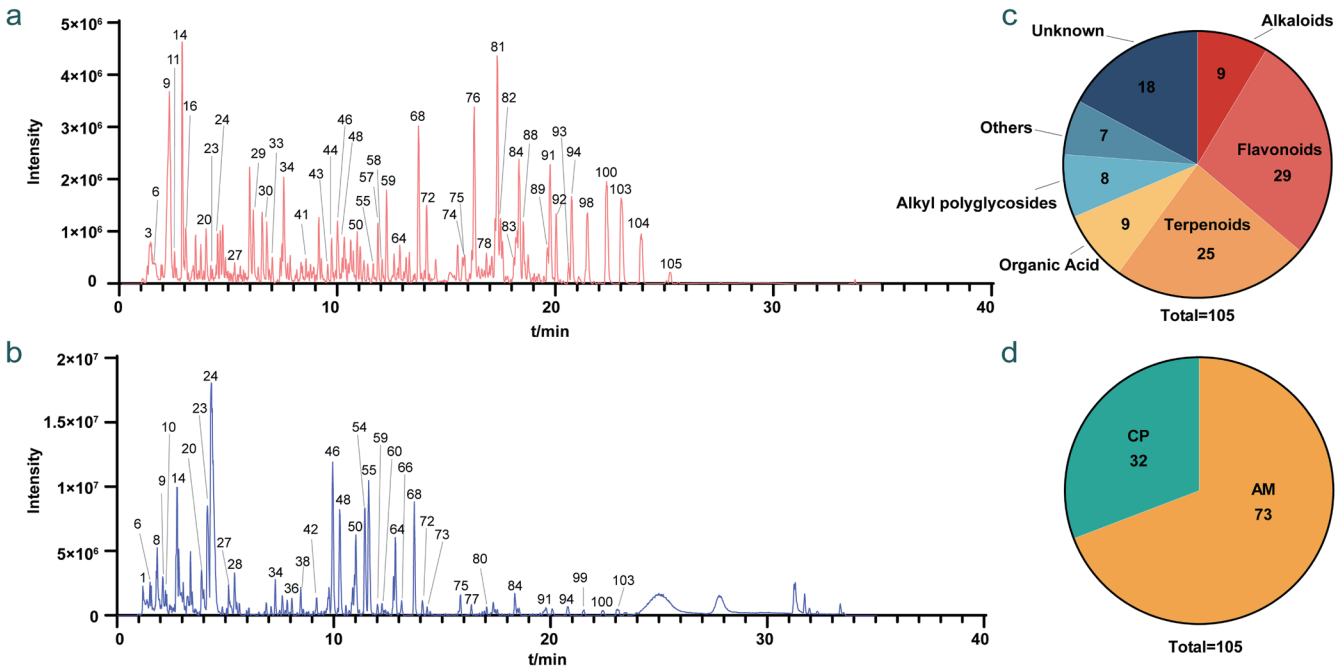

Fig. 1. Overall results of component identification of Shenqi Fuzheng (SQ) extract. (a) Total ion current chromatograms (TIC) of SQ extract by ultra-performance liquid chromatography-triple quadrupole time-of-flight mass spectrometry (UPLC-Triple-TOF/MS), negative ion mode; (b) TIC of SQ extract by UPLC-Triple-TOF/MS, positive ion mode; (c) Pie chart of the number of different types of compounds in SQ extract; (d) Pie chart of the number of compounds from different herbs in SQ extract. AM, *Radix Astragali*; CP, *Radix Codonopsis pilosula*.

is performed based on SQ extract data. The resulting peak list from the SQ extract is exported for component identification.

Identification of blood-absorbed components of SQ extract

The aligned feature table is exported for the analysis of blood components. The features of plasma samples from the control and drug groups are aligned with those of the SQ extract. Peaks are considered blood components if the peak area in the drug group is more than three times that in the control group and exceeds 1,000 in area. Peaks with retention times (RTs) between 2 m and 23 m are selected for further analysis. The blood components are identified based on an m/z error of less than 0.01 and an RT error of less than 0.01.

Results

One hundred and five chemical constituents of SQ extract are identified

The SQ extract is analyzed using the UPLC-Triple-TOF/MS method, resulting in positive and negative total ion chromatograms (Fig. 1a, b). Based on the precursor m/z and mass spectral fragmentation patterns, a total of 105 compounds are identified (Table 1), including 25 terpenoids, 29 flavonoids, eight alkyl polyglucosides, nine alkaloids, nine organic acids, and other compounds (Fig. 1c). Most prominent components of SQ are identified, with 10 compounds confirmed using reference standards. The origin of the compounds is also determined, with 73 isolated from *Radix Astragali* and 32 from *Radix Codonopsis pilosula* (Fig. 1d).

Terpenoids and their fragmentation patterns

Terpenoids primarily originate from *Radix Astragali*, including compounds such as Astragaloside IV, Astragaloside III, Astragaloside II, Isoastragaloside II, Astragaloside I, Isoastragaloside I, and Cycloaraloside E. For example, the fragmentation pattern of compound 80 is analyzed. The RT for compound 80 is 17.022 m. A $[M+H]^+$ peak with m/z of 815.4767 is observed in positive ion mode, suggesting a molecular formula of $C_{42}H_{70}O_{15}$. The secondary fragment ions detected are 143.10596, 437.34198, 455.35086, 815.47998, 419.32819, and 473.35938. Based on these data, compound 80 is assumed to be Cycloaraloside E, and its possible fragmentation pattern is illustrated in Figure 2.

Alkaloids and their fragmentation patterns

Alkaloids primarily originate from *Radix Codonopsis pilosula* and are detected in positive ion mode, including compounds such as Codonopsine, (2R,3R,4R,5R)-2-(hydroxymethyl)-5-(4-methoxyphenyl)-1-methylpyrrolidine-3,4-diol, Radicamine A, and Codonopsinol C. For example, the fragmentation pattern of compound 24 is analyzed. The RT for compound 24 is 4.34 m. A $[M+H]^+$ peak with m/z of 268.1536 is observed in positive ion mode, suggesting a molecular formula of $C_{14}H_{21}NO_4$. The secondary fragment ions detected are 88.08239, 58.06517, and 121.06402. Based on these data, compound 24 is assumed to be Codonopsine, and its possible fragmentation pattern is shown in Figure 3.

Flavonoids and their fragmentation patterns

Flavonoids primarily originate from *Radix Astragali*, including compounds such as Narcissin, Rhamnocitrin, Calycosin-7-O-β-D-glucopyranoside, Calycosin, and Ononin. For example, the fragmentation pattern of compound 64 is analyzed. The RT for compound 64 is 12.818 m. A $[M+FA-H]^-$ peak with m/z of 475.1247 is observed in negative ion mode, suggesting a molecular formula of

Table 1. Characterization of constituents in Shenqi Fuzheng (SQ) extract by ultra-performance liquid chromatography-triple quadrupole time-of-flight mass spectrometry (UPLC-Triple-TOF/MS)

No	Rt	Mz	Adduct	ppm	Formula	Name	MS/MS	Source
1	1.157	131.0468	$[M-H]^-$	−8.64	$C_4H_8N_2O_3$	L-isoasparagine	72.00975, 58.03087, 70.02944, 114.01923	AM
2	1.215	179.0559	$[M-H]^-$	−1.87	$C_6H_{12}O_6$	α-D-glucopyranose	59.01412, 71.01325, 85.03016, 56.99766, 55.01833	AM
3[b]	1.344	341.1073	$[M-H]^-$	3.20	$C_{12}H_{22}O_{11}$	Sucrose	59.01402, 71.01314, 89.02369, 101.02446, 113.02393	AM
4	1.441	116.0706	$[M+H]^+$	−4.77	$C_5H_9NO_2$	D-prolin	70.06343, 68.04769, 53.03716, 69.85431	AM
5	1.475	115.0038	$[M-H]^-$	−5.78	$C_4H_4O_4$	Maleic acid	71.01428	AM
6[b]	1.577	118.086	$[M+H]^+$	−6.81	$C_5H_{11}NO_2$	L-valine	55.05266, 72.07752, 57.05698, 56.04929	AM
7[b]	1.651	607.1702	$[M-H]^-$	−6.42	$C_{28}H_{32}O_{15}$	Tanoside I	103.00355, 59.0140, 503.15948, 341.10361	AM
8	1.835	256.1189	$[M+H]^+$	1.57	$C_{12}H_{17}NO_5$	Radicamine A	60.04468, 137.05962, 90.05214, 177.05446, 122.03488	CP
9[b]	2.092	240.1237	$[M+H]^+$	0.48	$C_{12}H_{17}NO_4$	Codonopsinol C	74.05977, 56.04929, 107.0492, 147.0439	CP
10	2.213	400.1703	$[M+NH_4]^+$	−4.23	$C_{17}H_{22}N_2O_8$	Tryptophan-N-glucoside	256.12851, 164.08186, 70.06462, 178.09523, 400.16238	CP
11[b]	2.425	165.0533	$[M+H]^+$	−11.33	$C_9H_8O_3$	P-coumaric acid	77.03858, 95.04868, 123.04395, 119.04932, 91.05324	CP
12[b]	2.628	323.0987	$[M-H]^-$	−2.71	$C_{12}H_20O_10$	Astrabhotin A	59.01402, 57.03468, 161.04385, 89.02369, 101.02305	AM
13[b]	2.714	270.1324	$[M+H]^+$	−6.47	$C_{13}H_{19}NO_5$	(2R,3R,4R,5R)-2-(3-hydroxy-4-methoxyphenyl)-5-(hydroxymethyl)-1-methylpyrrolidine-3,4-Diol	74.06091, 56.04924, 137.0594, 104.07057	CP
14[b]	2.759	268.1048	$[M+H]^+$	0.82	$C_{10}H_{13}N_5O_4$	Adenosine	136.06146, 119.03542, 94.03931, 57.03361, 268.10248	CP
15[b]	2.793	323.0986	$[M-H]^-$	−2.40	$C_{12}H_{20}O_{10}$	Astrabhotin D	99.04639, 59.01508, 143.03584, 89.02498, 71.01429	AM
16[b]	2.94	430.1562	$[M+H]^+$	0.30	$C_{15}H_{27}NO_{13}$	3-nitropropyl β-D-gentiobioside	136.06142, 298.11609, 178.07237, 430.15854, 280.10345	AM
17	3.122	430.1565	$[M+H]^+$	1.00	$C_{15}H_{27}NO_{13}$	3-nitropropyl β-D-cellobioside	136.06149, 298.11386, 178.07062, 280.10361	AM
18	3.427	382.1576	$[M+H]^+$	5.36	$C_{24}H_{19}N_3O_2$	(−)-benzomalVIn A	238.11772, 382.15045, 164.0798, 346.14282	CP
19[b]	3.518	145.0491	$[M+H]^+$	−6.79	$C_6H_8O_4$	5-methoxy-5-hydroxymethyl-2-furanone	99.04464, 53.03816, 71.04856, 55.01726, 57.03367	CP
20	3.886	166.0853	$[M+NH_4]^+$	−9.06	$C_9H_8O_2$	P-hydroxy-cinnamaldehyde	103.05436, 120.08138, 77.04225, 91.05454, 51.02303	CP

(continued)

Table 1. *(continued)*

No	Rt	Mz	Adduct	ppm	Formula	Name	MS/MS	Source
21	3.930	164.0718	$[M-H]^-$	−3.94	$C_9H_{11}NO_2$	L-phenylalanine	103.05617, 72.00844, 147.04482, 77.03866	CP
22[b]	3.978	416.1895	$[M+H]^+$	−6.15	$C_{19}H_{29}NO_9$	Codonopsinol C-1-O-β-D-glucopyranosyl	74.05985, 254.13847, 85.02854, 236.11742	CP
23[b]	4.16	254.1379	$[M+H]^+$	−5.25	$C_{13}H_{19}NO_4$	(2R,3R,4R,5R)-2-(hydroxymethyl)-5-(4-methoxyphenyl)-1-methylpyrrolidine-3,4-diol	74.06337, 121.06381, 161.05861, 56.04927, 254.13811	CP
24[b]	4.34	268.1536	$[M+H]^+$	−4.79	$C_{14}H_{21}NO_4$	Codonopsine	88.08239, 58.06517, 121.06402	CP
25[b]	4.425	433.1358	$[M-H]^-$	−2.76	$C_{18}H_{26}O_{12}$	2-methoxyphenol-4-O-β-apiofuranosyl-(1->2)-β-glucopyranoside	124.01704, 139.04063, 123.00861, 433.13721, 161.04716	AM
26	5.181	288.1209	$[M+H]^+$	−9.32	$C_{16}H_{17}NO_4$	Lycorine	244.09819, 245.10431, 200.10519, 270.112	AM
27[b]	5.206	359.0983	$[M-H]^-$	−1.32	$C_{15}H_{20}O_{10}$	Glucosyringic acid	123.00882, 138.03238, 197.04686, 182.02252, 153.05643	AM
28	5.342	353.0867	$[M-H]^-$	1.59	$C_{16}H_{18}O_9$	4-caffeoylquinic acid	191.05753, 179.0349, 173.04358,	AM
29	6.063	625.1753	$[M+H]^+$	−2.50	$C_{28}H_{32}O_{16}$	Narcissin	301.07047, 463.12155, 269.04428, 241.04871, 213.05444	AM
30[a]	6.698	353.0895	$[M-H]^-$	−6.34	$C_{16}H_{18}O_9$	3-caffeoylquinic acid	191.05763, 85.03001, 127.04032, 93.03312, 173.04358	AM
31	6.818	417.1375	$[M-H]^-$	5.25	$C_{18}H_{26}O_{11}$	Benzyl-α-L-arabinopyranosyl (1→6)-β-D-glucopyranoside	152.01183, 109.02929, 153.01967, 108.0211	CP
32	6.84	217.0964	$[M+H]^+$	−6.00	$C_{12}H_{12}N_2O_2$	(R)-2,3,4,9-tetrahydro-1H-pyrido[3,4-β] indole-3-carboxylic acid	144.08022, 143.07207, 127.05397, 115.05291, 77.03866	CP
33	6.909	353.0888	$[M-H]^-$	−4.36	$C_{16}H_{18}O_9$	Scopolin	135.04498, 173.04694, 191.05725, 179.03651, 93.03429	AM
34[b]	7.467	239.0567	$[M+FA-H]^-$	−4.75	$C_{10}H_{10}O_4$	Ferulic acid	91.05617, 149.06158, 72.99396, 117.03547, 163.04095	AM
35[b]	7.496	447.1495	$[M+FA-H]^-$	1.69	$C_{18}H_{26}O_{10}$	(2R,3R,4S,5S,6R)-2-phenyl methoxy-6-[[(2S,3R,4S,5S)-3,4,5-trihydroxyoxan-2-Yl] oxymethyl] oxane-3,4,5-triol	401.14713, 269.10394, 59.0139, 161.0453, 101.02425	AM
36[b]	8.009	449.1097	$[M-H]^-$	−2.92	$C_{21}H_{22}O_{11}$	(±)-4-O-β-D-glucopyranosylmaesopsine	259.06137, 269.04675, 125.02501, 287.05817, 449.11191	AM
37	8.085	525.1984	$[M-H]^-$	−2.28	$C_{25}H_{34}O_{12}$	7R,8R-threo-4,7,9,9′-tetrahydroxy-3-methoxy-8-O-4′-neolignan-3′-O-β-D-glucopyranoside	167.07224, 149.06152, 179.07239, 315.12314, 165.05583	CP
38	8.556	463.123	$[M+H]^+$	−2.25	$C_{22}H_{22}O_{11}$	Kaempferol 7-methyl ether 3-O-β-D-glucopyranoside	301.07022, 269.04407, 241.04851, 213.05222, 253.08461	AM

(continued)

Table 1. *(continued)*

No	Rt	Mz	Adduct	ppm	Formula	Name	MS/MS	Source
39	8.569	219.0677	$[M-H]^-$	−8.97	$C_{12}H_{12}O_4$	Lanceolune B	129.09377, 143.07257, 72.99265, 157.08601, 113.09688	CP
40	8.571	301.0689	$[M+H]^+$	−7.69	$C_{16}H_{12}O_6$	Rhamnocitrin	301.07022, 213.05428, 283.1066, 167.0602, 269.04407	AM
41	8.599	461.1077	$[M-H]^-$	1.50	$C_{22}H_{22}O_{11}$	3′,5-dihydroxy-4′-methoxyisoflavone-7-O-β-D-glucopyranoside	299.05893, 284.03448, 461.1131, 255.03055, 283.02457	AM
42	9.084	325.0931	$[M-H]^-$	−2.32	$C_{15}H_{18}O_8$	[(Z)-2-(β-glucopyranosyloxy)]-3-phenylpropenoic acid	119.05143, 117.03549, 101.03994, 91.05484, 163.04099	CP
43	9.526	609.179	$[M+H]^+$	−4.84	$C_{28}H_{32}O_{15}$	Chrysoeriol-7-O-β-D-glucopyranosyl-4-O-α-L-rhamnopyranoside	285.07657, 270.04977, 253.04907, 609.18884, 225.05264	AM
44[b]	9.651	444.2426	$[M+NH_4]^+$	−4.25	$C_{18}H_{34}O_{11}$	Hexyl-β-getiobioside	85.02848, 145.04947, 163.05962, 127.03801, 97.02808	CP
44[b]	9.673	471.2087	$[M+FA-H]^-$	−1.97	$C_{18}H_{34}O_{11}$	Hexyl-β-getiobioside	425.20444, 263.15073, 101.02417, 161.04697, 71.01411	CP
45	9.688	469.1335	$[M-H]^-$	2.36	$C_{21}H_{26}O_{12}$	3-{{6-O-[(2E)-3-(4-hydroxyphenyl)-1-oxoprop-2-En-1-Yl]-β-D-glucopyranosyl} oxy}-3-methyl glutaric acid	99.04629, 265.07318, 163.04085, 143.03571, 205.05055	CP
46[a, b]	9.93	447.1276	$[M+H]^+$	−3.41	$C_{22}H_{22}O_{10}$	Calycosin-7-O-β-D-glucopyranoside	285.0766, 270.05212, 253.0491, 225.05479, 137.02184	AM
46[a, b]	9.944	491.1194	$[M+FA-H]^-$	−0.91	$C_{22}H_{22}O_{10}$	Calycosin-7-O-β-D-glucopyranoside	283.06393, 268.03796, 211.04095, 239.03506	AM
47[b]	9.973	425.2028	$[M-H]^-$	−1.20	$C_{18}H_{34}O_{11}$	Hexyl β-sophoroside	263.15097, 59.01391, 101.02285, 71.01418, 113.02371	CP
48[b]	10.258	223.0625	$[M-H]^-$	−8.29	$C_{11}H_{12}O_5$	2-oxopropyl 3-hydroxy-4-methoxybenzoate	91.05593, 161.06116, 163.04233, 133.06561, 87.00856	CP
49	10.754	479.1565	$[M-H]^-$	−2.42	$C_{23}H_{28}O_{11}$	(3R,4R)-4,7-hydroxy-2′,3′-dimethoxyisoflavane-4′-O-β-D-glucoside	317.10544, 121.0302, 299.09201, 180.04138, 137.02386	AM
50	10.833	576.2635	$[M+NH_4]^+$	−3.68	$C_{26}H_{38}O_{13}$	Lobetyolinin	199.11131, 155.08499, 129.06955, 128.06142, 153.0695	CP
50	10.860	603.2292	$[M+FA-H]^-$	−0.50	$C_{26}H_{38}O_{13}$	Lobetyolinin	179.05701, 89.02474, 323.099, 119.0358, 221.06808	CP
51	11.131	671.2161	$[M+FA-H]^-$	3.92	$C_{29}H_{38}O_{15}$	Isomucronulatol 7,2′-Di-O-glucoside	301.10974, 463.16278, 286.08548, 135.0451, 121.02888	AM
52	11.161	261.1354	$[M-H]^-$	−6.07	$C_{12}H_{22}O_6$	(2R,3R,4S,5S,6R)-2-[((Z)-hex-3-enyl) oxy]-6-hydroxymethyl-tetrahydro-pyran-3,4,5-triol	125.09717, 187.09991, 97.06568, 123.08187, 169.08807	CP

(continued)

Table 1. *(continued)*

No	Rt	Mz	Adduct	ppm	Formula	Name	MS/MS	Source
53	11.329	598.2453	$[M+NH_4]^+$	−7.80	$C_{28}H_{36}O_{13}$	(+)-Syringaresinol O-β-D-glucopyranoside	205.08554, 265.10785, 173.05911, 217.08583, 167.06958	AM
54	11.528	533.1263	$[M+H]^+$	−6.04	$C_{25}H_{24}O_{13}$	6″-O-malonate-calycosin-7-O-β-D-glucoside	285.07458, 270.05243, 533.12842, 253.04942, 225.05505	AM
55[b]	11.544	463.1213	$[M+H]^+$	−5.92	$C_{22}H_{22}O_{11}$	Pratensein 7-O-glucopyranoside	301.07086, 286.0477, 269.04462, 241.049, 153.01735	AM
56[b]	11.634	287.0892	$[M+H]^+$	−9.58	$C_{16}H_{14}O_5$	Homobutein	153.05527, 138.02975, 110.03438, 147.04218, 125.05885	AM
57[b]	11.840	137.024	$[M-H]^-$	−0.95	$C_7H_6O_3$	4-Hydroxy-benzoic acid	93.03554, 65.03995, 75.0238, 137.02219, 67.01903	CP
58	12.006	441.1765	$[M+FA-H]^-$	−0.96	$C_{20}H_{28}O_8$	2-[(4E,12E)-1,7-dihydroxytetradeca-4,12-dien-8,10-diyn-6-Yl] oxy-6-(hydroxymethyl) oxane-3,4,5-triol	143.07272, 185.0995, 159.08182, 59.01288, 89.02492	CP
59[a, b]	12.196	414.2119	$[M+NH_4]^+$	−2.16	$C_{20}H_{28}O_8$	Lobetyolin	128.06136, 155.08492, 129.06949, 199.11124, 153.06944	CP
59[a, b]	12.216	441.1758	$[M+FA-H]^-$	0.62	$C_{20}H_{28}O_8$	Lobetyolin	143.07217, 159.08121, 185.0988, 59.01373, 89.0259	CP
60	12.216	443.1902	$[M+FA-H]^-$	3.44	$C_{20}H_{30}O_8$	Cordifolioidyne B	59.01373, 89.02458, 71.01397, 119.03405, 217.12573	CP
61	12.216	179.0569	$[M-H]^-$	−7.46	$C_6H_{12}O_6$	β-D-glucose	59.01481, 71.01279	AM
62	12.305	391.1891	$[M-H]^-$	4.69	$C_{25}H_{28}O_4$	Glabrol	79.95785, 391.18256, 263.09576, 59.01379, 71.01403	AM
63	12.727	489.1368	$[M+H]^+$	−5.91	$C_{24}H_{24}O_{11}$	6″-O-acetylcalycosin-7-O-β-D-glucopyranoside	285.07687, 270.05234, 253.04935, 225.05499, 137.02361	AM
64	12.804	431.1338	$[M+H]^+$	−0.95	$C_{22}H_{22}O_9$	Ononin	269.08118, 213.08931, 237.05499, 253.04909	AM
64	12.818	475.1247	$[M+FA-H]^-$	−1.39	$C_{22}H_{22}O_9$	Ononin	267.06595, 251.03471, 135.00726	AM
65	12.804	269.0791	$[M+H]^+$	−8.49	$C_{16}H_{12}O_4$	7-hydroxy-3-(4-methoxy-phenyl)-chromen-4-on	269.08142, 197.05923, 253.04932, 237.05521, 226.0591	AM
65	12.818	267.0674	$[M-H]^-$	−6.23	$C_{16}H_{12}O_4$	7-hydroxy-3-(4-methoxy-phenyl)-chromen-4-on	252.04385, 223.04179, 195.04605, 251.03471, 132.02257	AM
66	13.098	301.1057	$[M+H]^+$	−6.31	$C_{17}H_{16}O_5$	(−)-6Ar,11Ar-dihydro-3-hydroxy-9,10-dimethoxy-6H-benzofuro<3,2-C><1>-benzopyran	167.06935, 152.04739, 134.03592, 105.03297, 106.0416	AM
67	13.676	301.106	$[M+H]^+$	−5.31	$C_{17}H_{16}O_5$	2,4-dihydroxy-3,4-dimethoxychalcone	167.07112, 134.03589, 152.04735, 105.03294, 106.04013	AM

(continued)

Table 1. *(continued)*

No	Rt	Mz	Adduct	ppm	Formula	Name	MS/MS	Source
68[b]	13.676	463.1571	$[M+H]^+$	−7.18	$C_{23}H_{26}O_{10}$	Methylnissolin-3-O-glucoside	167.07117, 301.10693, 152.04565, 134.03593, 191.06966	AM
69	13.676	167.07	$[M+H]^+$	−4.91	$C_9H_{10}O_3$	α-acetylorcinol	78.04539, 77.03735, 105.02865, 106.03582, 134.0343	AM
70	13.686	507.1522	$[M+FA-H]^-$	−3.84	$C_{23}H_{26}O_{10}$	(6Ar,11Ar)-9,10-dimethoxypterocarpan-3-β-D-glucoside	299.09467, 269.04861, 284.06934, 241.05037, 507.15808	AM
71[b]	13.819	509.1649	$[M+FA-H]^-$	1.97	$C_{23}H_{28}O_{10}$	Isomucronulatol 7-O-glucoside	301.1088, 286.08459, 135.04466, 271.06082, 109.03046	AM
72	14.058	463.1595	$[M-H]^-$	2.00	$C_{23}H_{28}O_{10}$	(3R)-7,2′-dihydroxy-3′,4′-dimethoxyisoflavan-7-O-β-D-glucoside	301.10919, 121.03019, 286.08496, 135.04646, 271.06348	AM
72	14.063	482.2001	$[M+NH_4]^+$	−5.23	$C_{23}H_{28}O_{10}$	(3R)-7,2′-dihydroxy-3′,4′-dimethoxyisoflavan-7-O-β-D-glucoside	167.06961, 123.04414, 303.12402, 133.06383, 161.05898	AM
73[a]	14.266	285.0746	$[M+H]^+$	−5.96	$C_{16}H_{12}O_5$	Calycosin	285.07648, 270.052, 213.0544, 253.04901, 225.0547	AM
73[a]	14.266	283.0603	$[M-H]^-$	1.24	$C_{16}H_{12}O_5$	Calycosin	268.03766, 211.04071, 239.03696, 195.04593, 240.04349	AM
74	15.72	473.1434	$[M+H]^+$	−2.91	$C_{24}H_{24}O_{10}$	6″-O-acetyl-7-(β-D-glucopyranosyloxy)-3-(4-methoxyphenyl) chromen-4-one	269.08118, 254.05779, 213.08931, 237.05283, 253.04684	AM
75	15.790	991.5134	$[M+FA-H]^-$	−2.03	$C_{47}H_{78}O_{19}$	(3β,6α,16B,20R,24S)-20,24-epoxy-16-hydroxy-3-(β-D-xylopyranosyloxy)-9,19-cyclolanostane-6,25-diyl bis[β-D-glucopyranoside]	945.51074, 991.52429, 946.5174, 783.45966, 89.02455	AM
75	15.797	947.5188	$[M+H]^+$	−2.91	$C_{47}H_{78}O_{19}$	(3β,6α,16β,20R,24S)-20,24-epoxy-16-hydroxy-3-(β-D-xylopyranosyloxy)-9,19-cyclolanostane-6,25-diyl bis[β-D-glucopyranoside]	143.10579, 437.34149, 455.35037, 947.5177, 419.3306	AM
76	16.309	301.1058	$[M+H]^+$	−5.98	$C_{17}H_{16}O_5$	(−)-Naringenin 4′,7-dimethyl ether	167.06947, 134.03439, 152.04576, 106.04023, 105.0316	AM
77	16.559	829.4584	$[M+FA-H]^-$	0.20	$C_{41}H_{68}O_{14}$	Isoastragaloside IV	783.46082, 829.46387, 161.04681, 101.02409	AM
78	16.806	457.3654	$[M+H]^+$	−6.06	$C_{30}H_{48}O_3$	Ursolic acid	421.34647, 439.35599, 457.36679, 109.09957, 127.1095	CP
79[b]	16.961	831.4748	$[M+FA-H]^-$	−0.70	$C_{41}H_{70}O_{14}$	Cyclocanthoside E	785.47174, 831.4762, 491.37457, 623.41815	AM
80	17.020	859.4708	$[M+FA-H]^-$	−1.94	$C_{42}H_{70}O_{15}$	Cycloaraloside E	813.474, 859.47656, 651.41406, 161.04691	AM
80	17.022	815.4767	$[M+H]^+$	−3.19	$C_{42}H_{70}O_{15}$	Cycloaraloside E	143.10596, 437.34198, 455.35086, 815.47998, 419.32819, 473.35938	AM

(continued)

Table 1. *(continued)*

No	Rt	Mz	Adduct	ppm	Formula	Name	MS/MS	Source
81	17.315	329.2343	$[M-H]^-$	−4.56	$C_{18}H_{34}O_5$	5,6,9-trihydroxy-octadec-7-enoic acid	211.1349, 329.23553, 229.14568, 171.10298, 183.13995	CP
82[b]	17.401	991.5098	$[M+FA-H]^-$	1.60	$C_{47}H_{78}O_{19}$	Astragaloside V	945.50763, 991.51666, 783.45673, 946.51855, 161.04498	AM
83[b]	18.010	871.4667	$[M+FA-H]^-$	2.79	$C_{43}H_{70}O_{15}$	Astragaloside II	825.47247, 765.45331, 783.46143, 871.47253	AM
84[a, b]	18.318	829.4597	$[M+FA-H]^-$	−1.37	$C_{41}H_{68}O_{14}$	Astragaloside IV	829.46796, 783.46088, 179.05688, 89.02336, 119.03419	AM
85	18.325	473.3584	$[M+H]^+$	−9.90	$C_{30}H_{48}O_4$	Choushenpilosulyne C	123.11601, 437.34207, 143.10597, 455.35095, 473.36249	CP
86	18.43	301.1064	$[M+H]^+$	−3.99	$C_{17}H_{16}O_5$	7-hydroxy-2′-methoxy-4′,5-methylenedioxyisoflavan	167.06973, 152.04601, 134.03461, 105.03321	AM
87	18.507	473.361	$[M+H]^+$	−4.40	$C_{30}H_{48}O_4$	Dihydrocycloorbigenin A	143.1041, 437.3385, 123.11428, 125.09369, 455.34729	AM
88[a]	18.507	829.4607	$[M+FA-H]^-$	−2.57	$C_{41}H_{68}O_{14}$	Astragaloside III	783.45923, 829.47021, 161.04649, 101.02529, 489.35767	AM
89	19.577	911.504	$[M-H]^-$	−3.92	$C_{47}H_{76}O_{17}$	Astragaloside VIII	911.51025, 893.49237, 205.07166, 615.39325, 163.06155	AM
90	19.621	941.5126	$[M-H]^-$	−1.70	$C_{48}H_{78}O_{18}$	Soyasaponin I	941.51917, 923.50861, 205.06972, 163.06161, 615.39349	AM
90	19.672	943.5236	$[M+H]^+$	−3.23	$C_{48}H_{78}O_{18}$	Soyasaponin I	441.37225, 423.36148, 943.52722, 599.39429, 797.46985	AM
91	19.736	873.4797	$[M+FA-H]^-$	5.82	$C_{43}H_{72}O_{15}$	Agroastragaloside II	873.48694, 59.01371, 767.45422	AM
92	20.04	473.3611	$[M+H]^+$	−4.19	$C_{30}H_{48}O_4$	3β,21α-dihydroxyolean-12-ene-28-oic acid	143.10579, 437.34149, 123.11586, 455.35037, 125.09371	AM
93[b]	20.591	915.4984	$[M-H]^-$	−3.34	$C_{46}H_{76}O_{18}$	3-O-β [α-L-arabinopyranosyl (1->2) β-D-xylopyranosyl]-6-O-β-D-glucopyranosyl-20(R),24(S)-epoxy-3β,6α,16β,25-tetrahydroxycycloartane	915.50037, 869.49237, 59.01362, 827.48022, 809.47772	AM
94[a, b]	20.736	871.4714	$[M+FA-H]^-$	−2.60	$C_{43}H_{70}O_{15}$	Isoastragalosides II	871.47644, 825.46429, 59.01355, 765.44946, 179.05612	AM
95[b]	20.752	473.361	$[M+H]^+$	−4.40	$C_{30}H_{48}O_4$	Astragalene	123.11444, 437.34201, 143.10596, 125.09385, 141.12675	AM
96	21.073	939.4927	$[M-H]^-$	2.82	$C_{48}H_{76}O_{18}$	Dehydrosoyasaponin I	939.49957, 921.49567, 163.06174, 205.07591, 613.37463	AM

(continued)

Table 1. *(continued)*

No	Rt	Mz	Adduct	ppm	Formula	Name	MS/MS	Source
97	21.384	915.497	$[M-H]^-$	−1.81	$C_{46}H_{76}O_{18}$	3-O-[α-L-arabinopyranosyl-(1->2)-β-D-xylanopyranosyl]-6-O-β-D-glucopyranosyl-3β,6α,16β,24α-tetrahydroxy-20(R),25-epoxycycloartane	915.50958, 869.49304, 59.01366, 809.48236, 827.48895	AM
98[b]	21.456	871.4705	$[M+FA-H]^-$	−1.57	$C_{43}H_{70}O_{15}$	16-O-acetyl-20R,24S-epoxycycloartan-3Gammab,6α,16β,25-tetraol 3-O-β-D-xylopyranoside 6-O-β-D-glucopyranoside	871.47742, 825.47327, 59.01361, 765.45032, 179.0563	AM
98[b]	21.477	827.4728	$[M+H]^+$	−7.86	$C_{43}H_{70}O_{15}$	16-O-acetyl-20R,24S-epoxycycloartan-3Gammab,6α,16β,25-tetraol 3-O-β-D-xylopyranoside 6-O-β-D-glucopyranoside	143.10574, 437.34137, 175.05865, 125.09525, 455.35025	AM
99[b]	21.507	231.138	$[M+H]^+$	−2.18	$C_{15}H_{18}O_2$	Epi-curzerenone	77.03749, 105.06916, 91.05341, 128.06143, 163.07605	CP
100[a, b]	22.342	913.4767	$[M+FA-H]^-$	3.28	$C_{45}H_{72}O_{16}$	Astragaloside I	913.49219, 867.48151, 59.01476, 825.46606, 807.46564	AM
101	22.342	915.4899	$[M+FA-H]^-$	5.95	$C_{45}H_{74}O_{16}$	Agroastragaloside I	915.49707, 869.49329, 59.01368, 827.47699, 914.49438	AM
102	22.359	689.4241	$[M+H]^+$	−3.44	$C_{39}H_{60}O_{10}$	6α-acetoxy-23α-ethoxy-16β,23(R)-epoxy-24,25,26,27-tetranor-9,19-cyclolanosta-3-O-[β-D-(4′-trans-2-butenoyl) xylopyranoside]	157.0484, 143.10567, 217.06918, 437.33817, 689.42773	AM
103[a, b]	23.032	913.4801	$[M+FA-H]^-$	−0.44	$C_{45}H_{72}O_{16}$	Isoastragaloside I	913.49487, 867.47998, 59.01466, 825.46869, 807.46027	AM
103[a, b]	23.037	869.4901	$[M+H]^+$	0.27	$C_{45}H_{72}O_{16}$	Isoastragaloside I	143.1059, 217.06953, 139.03867, 157.04866, 199.05997	AM
104	23.942	915.4902	$[M-H]^-$	5.62	$C_{46}H_{76}O_{18}$	3-O-β-D-xylopyranosyl-6-O-β-D-xylopyranosyl-25-O-β-D-glucopyranosyl-(20R,24S)-epoxy-3β,6α,25-tetrahydroxycycloartane	915.49835, 869.49048, 59.01457, 914.49988, 809.46393	AM
105	25.280	955.4918	$[M-H]^-$	−1.61	$C_{48}H_{76}O_{19}$	3-O-α-L-rhamnopyranosyl(1<*>2)-β-D-galactopyranosyl(1<*>2)-β-D-glucuronopyranosyl complogenin	955.49377, 909.48663, 59.01353, 867.4917, 161.04428	AM

[a]standard comparison compound; [b]blood entry component; AM, *Radix Astragali*; CP, *Radix Codonopsis pilosula*.

$C_{22}H_{22}O_9$. The secondary fragment ions detected are 267.06595, 251.03471, and 135.00726. Based on these data, compound 64 is assumed to be Ononin, and its possible fragmentation pattern is shown in Figure 4.

Alkyl polyglucosides and their fragmentation patterns

Alkyl polyglycosides primarily originate from *Radix Codonopsis pilosula*, including compounds such as Hexyl-β-getiobioside, Lobetyolinin, Lobetyolin, and Cordifolioidyne B. For example,

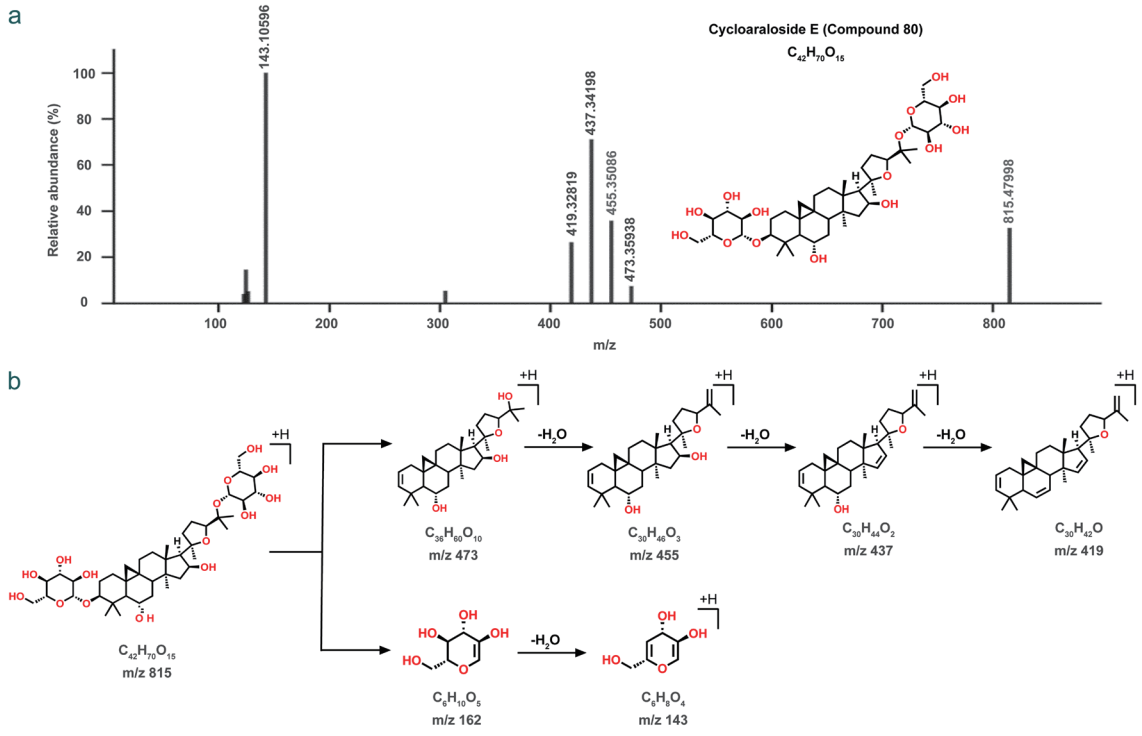

Fig. 2. Fragmentation pattern of Cycloaraloside E (Compound 80). m/z, mass-to-charge ratio.

the fragmentation pattern of compound 44 is analyzed. The RT for compound 44 is 9.673 m. A $[M+H]^+$ peak with m/z of 471.2087 is observed in positive ion mode, suggesting a molecular formula of $C_{18}H_{34}O_{11}$. The secondary fragment ions detected are 425.20444, 263.15073, 101.02417, 161.04697, and 71.01411. Based on these data, compound 44 is assumed to be Hexyl-β-getiobioside, and its

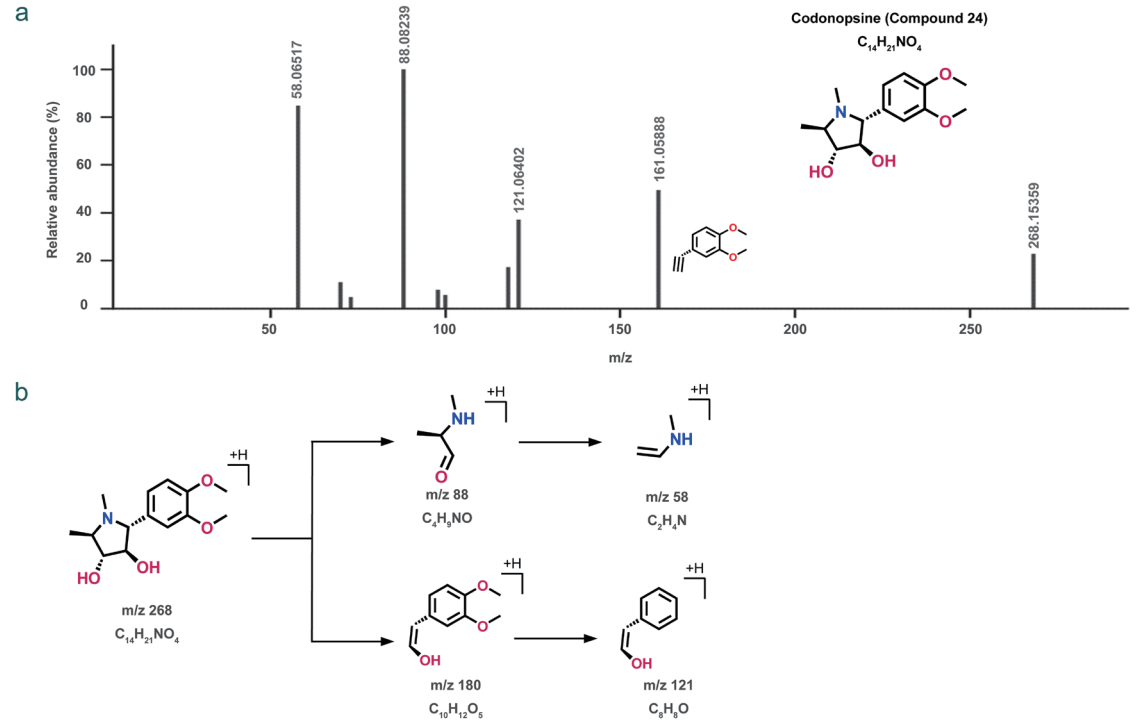

Fig. 3. Fragmentation pattern of Codonopsine (Compound 24). m/z, mass-to-charge ratio.

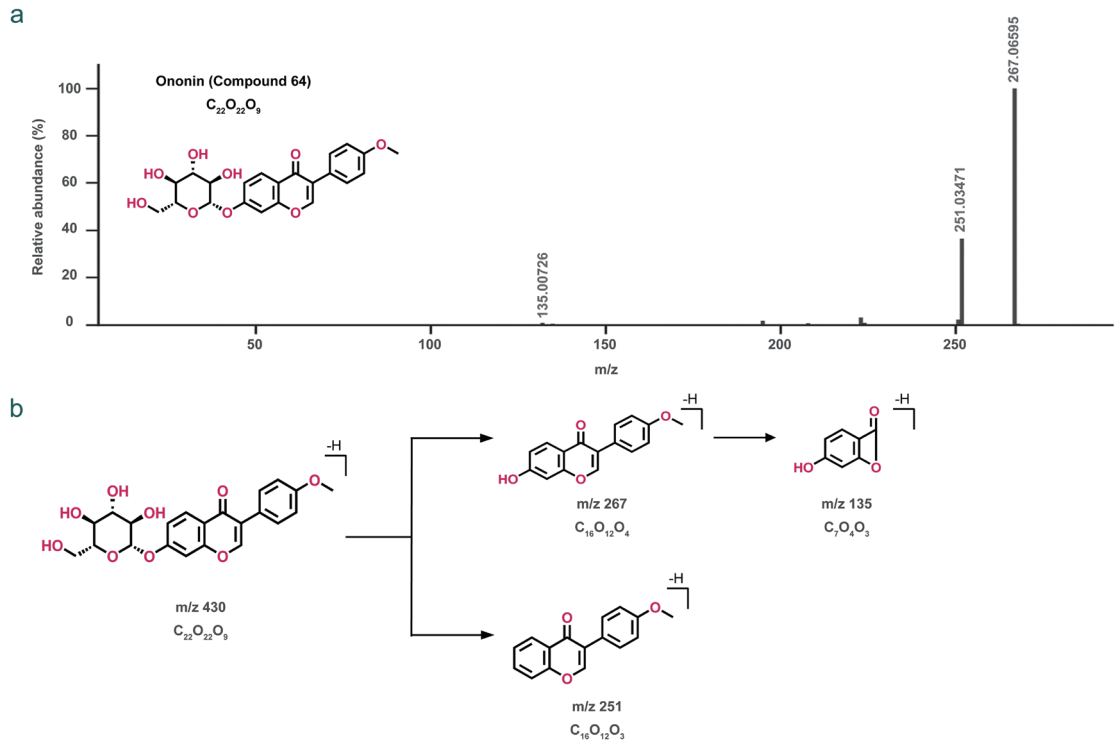

Fig. 4. Fragmentation pattern of Ononin (Compound 64). m/z, mass-to-charge ratio.

possible fragmentation pattern is shown in Figure 5.

Organic acids and their fragmentation patterns

Organic acids primarily originate from both *Radix Codonopsis pilosula* and *Radix Astragali*, including compounds such as Maleic acid, P-coumaric acid, Glucosyringic acid, and 4-caffeoylquinic acid. For example, the fragmentation pattern of compound 28 is analyzed. The RT for compound 28 is 5.342 m. A $[M-H]^-$ peak with m/z of 353.0867 is observed in the positive ion mode, suggesting a molecular formula of $C_{16}H_{18}O_9$. The secondary fragment ions detected are 191.05753, 179.0349, and 173.04358. Based on these data, compound 28 is assumed to be 4-caffeoylquinic acid, and its possible fragmentation pattern is shown in Figure 6.

Others

Other constituents include carbohydrates (e.g., Sucrose, β-D-glucose) and amino acids (e.g., L-isoasparagine, D-proline, and L-valine). These do not belong to secondary metabolites, so their fragmentation patterns are not detailed.

Forty blood-absorbed components of SQ extract are identified

The UPLC-Triple-TOF/MS method is used to analyze the plasma of rats in control and drug groups. Positive and negative total ion chromatograms are obtained (Fig. 7a, b). A total of 40 prototype compounds are identified (Table 1), including 10 terpenoids, six flavonoids, two alkyl polyglucosides, five alkaloids, four organic acids, and other compounds (Fig. 7c). Of these, 26 compounds are isolated from *Radix Astragali* and 14 from *Radix Codonopsis pilosula* (Fig. 7d).

The average amount of compounds in the blood at different time points is shown (Fig. 7e). The contents of L-valine (Compound 6), P-coumaric acid (Compound 11), and Ferulic acid (Compound 34) are the highest, indicating that organic and amino acids are important components of SQ extract. The relative contents of blood compounds are calculated at different time points (Fig. 7f). Astragalosides, such as Astragaloside V (Compound 82), Astragaloside II (Compound 83), Astragaloside IV (Compound 84), Isoastragalosides II (Compound 94), and Isoastragaloside I (Compound 103), are found to be more abundant in the blood within 5 m of administration and less abundant after 15 m, with Astragaloside IV being the most prevalent (Fig. 7e). Flavonoids (e.g., Compounds 36, 55, 56) enter the bloodstream in large quantities between 15 m and 30 m, while alkaloids (e.g., compounds 9, 13, 24) increase significantly about 1 h after administration.

Discussion

UPLC-Triple-TOF/MS analysis reveals that the SQ extract contains a variety of chemical components, including flavonoids, terpenoids, alkaloids, alkyl polyglucosides, and organic acids. Several of these compounds are consistent with previous studies on the SQ injection.[12,13,22] Notably, classic constituents from the SQ formula, such as Ononin, Adenosine, Codonopsine, Lobetyolin, Pratensein 7-O-glucopyranoside, Calycosin, Calycosin-7-O-β-D-glucopyranoside, 9,10-dimethoxypterocarpane-3-O-β-D-glucopyranoside, Isomucronulatol 7-O-glucoside, and multiple Astragalosides, were detected. These compounds are mainly flavonoids and terpenoids, among which Calycosin-7-O-β-D-glucopyranoside, Lobetyolin, and several Astragalosides can be absorbed into the blood of rats. We also identified several new components in the SQ formula, such as Lobetyolinin, Cyclocanthoside E, and hexyl β-sophoroside, along with some alkaloids and organic acids. Alkaloids like Codonopsinol B and Codonopsinol C, as well as organic acids such as Ferulic acid and p-Coumaric acid, were detected in rat blood. Moreover, the sources of

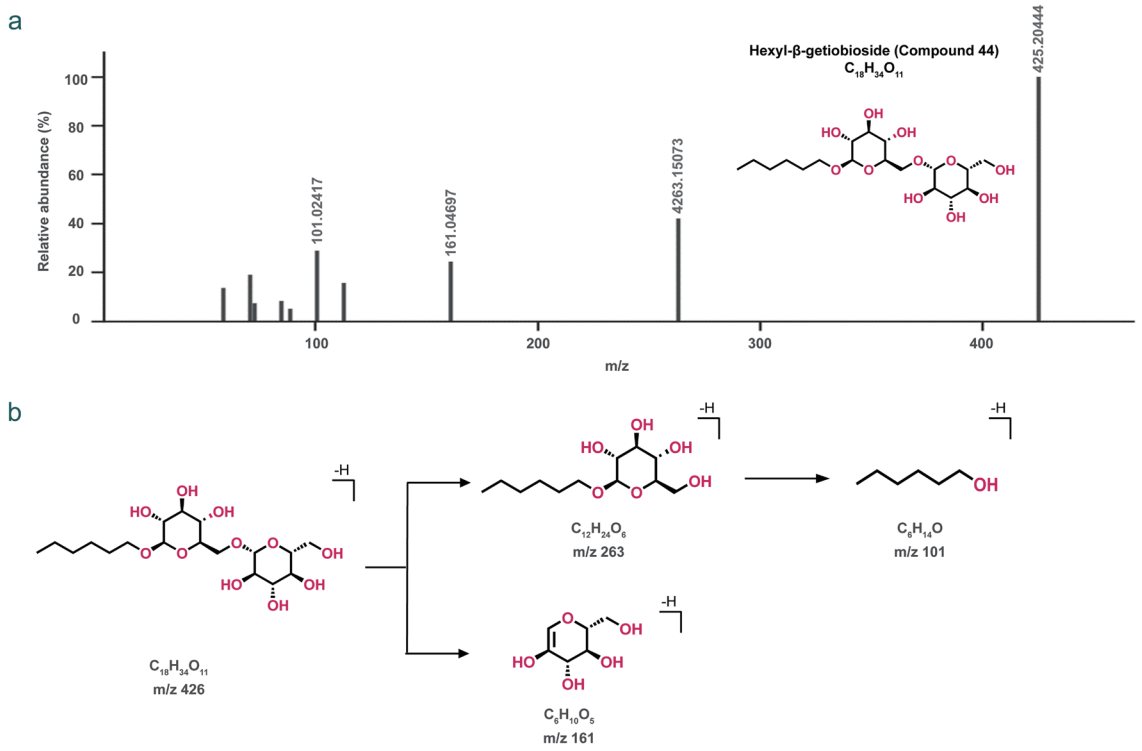

Fig. 5. Fragmentation pattern of Hexyl-β-getiobioside (Compound 44). m/z, mass-to-charge ratio.

these compounds were determined using existing databases.

A notable strength of this study is the analysis of compounds absorbed in rat blood at different time points following oral administration of the SQ extract, highlighting the drug's pharmacokinetic characteristics. Terpenoids, which are readily absorbed, accounted for 10 of the 40 components detected in the blood, with detec-

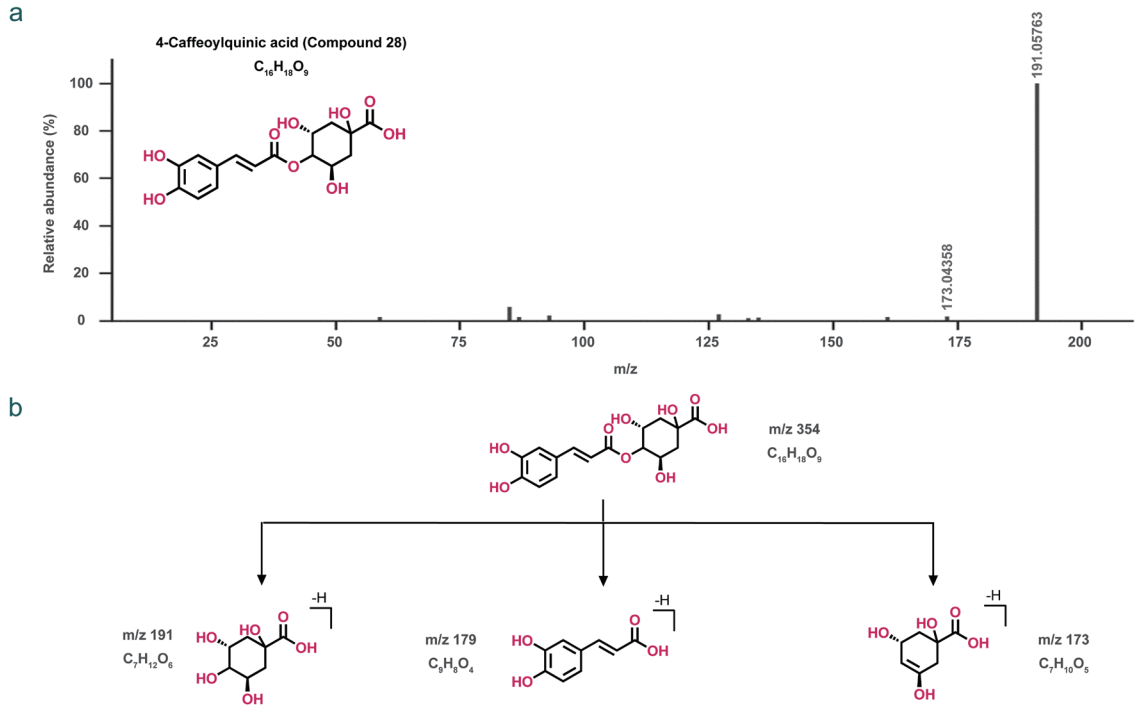

Fig. 6. Fragmentation pattern of 4-caffeoylquinic acid (Compound 28). m/z, mass-to-charge ratio.

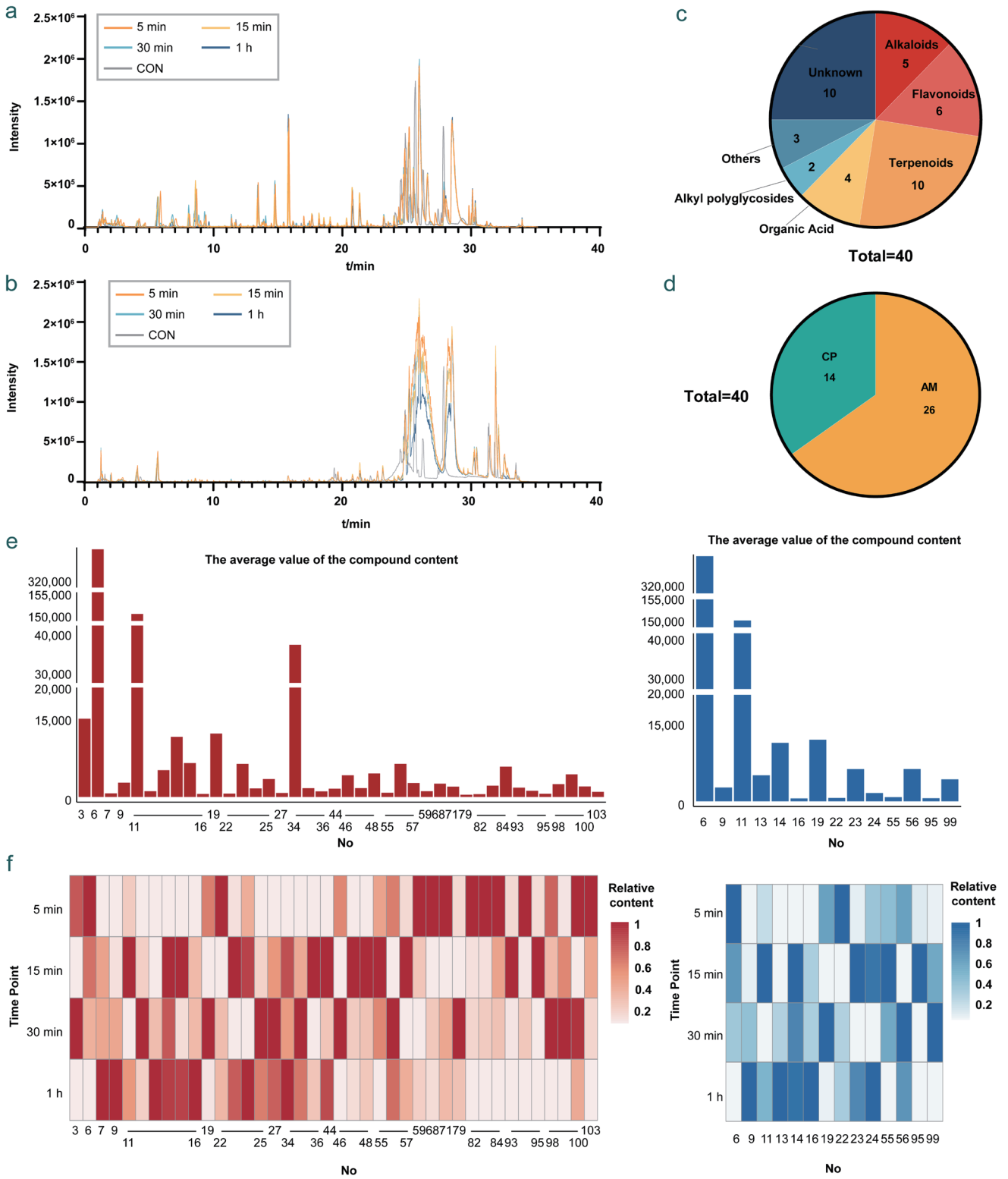

Fig. 7. Overall results of blood-absorbed component identification. (a) Total ion current chromatograms (TIC) of Shenqi Fuzheng (SQ) extract by ultra-performance liquid chromatography-triple quadrupole time-of-flight mass spectrometry (UPLC-Triple-TOF/MS), negative ion mode; (b) TIC of SQ extract by UPLC-Triple-TOF/MS, positive ion mode; (c) Pie chart of the number of different types of compounds in blood; (d) Pie chart of the number of compounds from different herbs in blood; (e) The average value of the content of the compounds, negative ion mode (left) and positive ion mode (right); (f) Heatmap of the relative content of blood compounds at different time points, negative ion mode (left) and positive ion mode (right). AM, *Radix Astragali*; CON, control; CP, *Radix Codonopsis pilosula*.

tion occurring within 5 m post-administration. These include compounds such as Astragaloside IV, Astragaloside V, and Astragaloside II, which are also rapidly metabolized. Additionally, alkaloids, organic acids, flavonoids, and alkyl polyglucosides were also detected in the blood, including Codonopsinol C, Calycosin-7-O-β-D-glucopyranoside, and Lobetyolin. These compounds typically appeared in the blood at 15 m post-administration, with some detectable even 1 h after ingestion. Understanding the pharmacokinetic properties is crucial for identifying the effective components of the SQ extract and optimizing their clinical efficacy.

The compounds that enter the blood are closely related to the efficacy of the SQ formula in TCM and modern medicine (Supplementary Table 1). As a traditional Qi-supplementing formula, SQ's blood-absorbed components enhance energy metabolism, regulate immune responses, resist inflammatory damage and oxidative stress, and promote cell regeneration or wound healing. For example, Calycosin-7-O-β-D-glucoside attenuates palmitate-induced lipid accumulation in hepatocytes through activation of the energy metabolism pathway,[23] Astragaloside II ameliorates mitochondrial dysfunction in diabetic rats,[24] Lobetyolin demonstrates protective effects against LPS-induced sepsis,[25] and Cyclocanthoside E stimulates growth *in vitro* and promotes wound healing *in vivo*.[26] In addition, the SQ formula helps enhance immune function and promote tumor treatment. Specifically, Astragaloside IV has been widely studied for its antitumor effects against colorectal,[27] lung cancer,[28] breast cancer,[29] and other cancers by promoting tumor cell apoptosis, inhibiting cell proliferation, improving the tumor immune microenvironment, and reducing chemotherapy resistance.[30,31] Additionally, several other compounds absorbed into the blood also contribute to cancer treatment. Astragaloside II inhibits autophagic flux and enhances the chemosensitivity of cisplatin in human cancer cells,[32] while Lobetyolin induces apoptosis in colon cancer cells by inhibiting glutamine metabolism.[33]

Despite the comprehensive analysis of the chemical composition and blood-absorbed constituents of the SQ extract, several limitations exist. First, the potential synergies among these components remain to be elucidated. Second, the therapeutic effects of the bioactive components in humans need validation through clinical trials. It is crucial to conduct in-depth studies on the interactions between these compounds and their impact on human health. Third, our utilization of UPLC-Triple-TOF/MS may not be sufficient. Significant progress has been made in the research of plant/herbal-derived exosomes.[34–38] Plant exosomes are complex biological samples containing proteins, lipids, nucleic acids, and other components.[35,37] Some existing studies have used UPLC-MS/MS to detect lipids, proteins, and metabolites in exosomes.[39,40] Compared to UPLC-MS/MS, UPLC-Triple-TOF/MS offers superior capabilities for qualitative and quantitative measurements, enabling the identification of complex mixtures and providing a more comprehensive analysis.[41] In the future, UPLC-Triple-TOF/MS may contribute to the multiple characterizations of the chemical and biological compositions of herbal medicine. Therefore, future studies should incorporate advanced techniques, such as transcriptomics, metabolomics, and proteomics,[42–45] to gain a deeper understanding of the mechanisms of action of these bioactive compounds. This knowledge could facilitate the development of more effective and targeted therapies based on the SQ formula.

Conclusions

This study successfully elucidates the chemical constituents of the SQ extract and identifies the compounds that can be absorbed into the bloodstream, offering new insights into their pharmacokinetics. These absorption components are closely related to the therapeutic effects of the SQ formula, especially in the fields of Qi supplementation and tumor treatment, which are key to both traditional and modern applications of the SQ formula.

Importantly, this work also promotes the application of UPLC-Triple-TOF/MS in the analysis of TCM compounds, showcasing the advantages of mass spectrometry in unraveling complex herbal formulations. We hope that our work encourages further exploration of this technique and helps to expand its application in herbal research.

In conclusion, this study enhances our understanding of the chemical and biologically active ingredients of SQ, providing a foundation for its continued use in TCM. Future research should focus on elucidating the pharmacological activities of the identified compounds and investigating their potential synergistic effects within the formulation.

Acknowledgments

The authors thank the High-Performance Computing Cluster of the Zhejiang University Innovation Center of the Yangtze River Delta for their technical support.

Funding

This work is supported by the National Natural Science Foundation of China (No. 82204772).

Conflict of interest

XHF and JL have been editorial board members of *Future Integrative Medicine* since March 2024. LFL and WHH are employees of Livzon Pharmaceutical Group Inc. This company has no conflicts of interest regarding the publication of this paper. The other authors report no conflict of interest in this work.

Author contributions

Research design, material preparation, writing and revision of the manuscript (MLW, MG, YNH, LFL, WHH), data collection (XL, ZWG, BJZ), conceptualization and supervision of the project (JL, XHF). All authors approve the final version of the manuscript.

Ethical statement

This study was carried out in accordance with the recommendations in the Regulations for the Administration of Affairs Concerning Experimental Animals and Guidelines for the Ethical Review of Laboratory Animal Welfare. The Animal Care and Use Committee of the Zhejiang University School of Medicine approved the animal experiments (Protocol Number: 22768). All surgery was performed under tribromoethanol, and all efforts were made to minimize suffering.

Data sharing statement

The data used to support the findings of this study are available from the corresponding author upon request.

References

[1] Huang K, Zhang P, Zhang Z, Youn JY, Wang C, Zhang H, *et al*. Traditional Chinese Medicine (TCM) in the treatment of COVID-19 and other viral infections: Efficacies and mechanisms. Pharmacol Ther 2021;225:107843. doi:10.1016/j.pharmthera.2021.107843, PMID: 33811957.

[2] Li S, Wu Z, Le W. Traditional Chinese medicine for dementia. Alzheimers Dement 2021;17(6):1066–1071. doi:10.1002/alz.12258, PMID:33682261.

[3] Efferth T, Li PC, Konkimalla VS, Kaina B. From traditional Chinese medicine to rational cancer therapy. Trends Mol Med 2007;13(8):353–361. doi:10.1016/j.molmed.2007.07.001, PMID:17644431.

[4] Dong J, Su SY, Wang MY, Zhan Z. Shenqi fuzheng, an injection concocted from Chinese medicinal herbs, combined with platinum-based chemotherapy for advanced non-small cell lung cancer: a systematic review. J Exp Clin Cancer Res 2010;29(1):137. doi:10.1186/1756-9966-29-137, PMID:20969765.

[5] Li W, Zhang Z, Berik E, Liu Y, Pei W, Chen S, *et al*. Energy preservation for skeletal muscles: Shenqi Fuzheng injection prevents tissue wasting and restores bioenergetic profiles in a mouse model of chemotherapy-induced cachexia. Phytomedicine 2024;125:155269. doi:10.1016/j.phymed.2023.155269, PMID:38237510.

[6] Yang J, Li Y, Chau CI, Shi J, Chen X, Hu H, *et al*. Efficacy and safety of traditional Chinese medicine for cancer-related fatigue: a systematic literature review of randomized controlled trials. Chin Med 2023;18(1):142. doi:10.1186/s13020-023-00849-y, PMID:37907925.

[7] Wang J, Tong X, Li P, Cao H, Su W. Immuno-enhancement effects of Shenqi Fuzheng Injection on cyclophosphamide-induced immunosuppression in Balb/c mice. J Ethnopharmacol 2012;139(3):788–795. doi:10.1016/j.jep.2011.12.019, PMID:22212503.

[8] Liao J, Hao C, Huang W, Shao X, Song Y, Liu L, *et al*. Network pharmacology study reveals energy metabolism and apoptosis pathways-mediated cardioprotective effects of Shenqi Fuzheng. J Ethnopharmacol 2018;227:155–165. doi:10.1016/j.jep.2018.08.029, PMID:30145173.

[9] Ma Y, Qi Y, Zhou Z, Yan Y, Chang J, Zhu X, *et al*. Shenqi Fuzheng injection modulates tumor fatty acid metabolism to downregulate MDSCs infiltration, enhancing PD-L1 antibody inhibition of intracranial growth in Melanoma. Phytomedicine 2024;122:155171. doi:10.1016/j.phymed.2023.155171, PMID:37925891.

[10] Cai YM, Zhang Y, Zhang PB, Zhen LM, Sun XJ, Wang ZL, *et al*. Neuroprotective effect of Shenqi Fuzheng injection pretreatment in aged rats with cerebral ischemia/reperfusion injury. Neural Regen Res 2016;11(1):94–100. doi:10.4103/1673-5374.175052, PMID:26981095.

[11] Du J, Cheng BC, Fu XQ, Su T, Li T, Guo H, *et al*. In vitro assays suggest Shenqi Fuzheng Injection has the potential to alter melanoma immune microenvironment. J Ethnopharmacol 2016;194:15–19. doi:10.1016/j.jep.2016.08.038, PMID:27566207.

[12] Li S, Zhu Z, Chen Z, Guo Z, Wang Y, Li X, *et al*. Network pharmacology-based investigation of the effects of Shenqi Fuzheng injection on glioma proliferation and migration via the SRC/PI3K/AKT signaling pathway. J Ethnopharmacol 2024;328:118128. doi:10.1016/j.jep.2024.118128, PMID:38561056.

[13] Wang J, Tong X, Li P, Liu M, Peng W, Cao H, *et al*. Bioactive components on immuno-enhancement effects in the traditional Chinese medicine Shenqi Fuzheng Injection based on relevance analysis between chemical HPLC fingerprints and in vivo biological effects. J Ethnopharmacol 2014;155(1):405–415. doi:10.1016/j.jep.2014.05.038, PMID:24950446.

[14] Zhu B, Li Z, Jin Z, Zhong Y, Lv T, Ge Z, *et al*. Knowledge-based in silico fragmentation and annotation of mass spectra for natural products with MassKG. Comput Struct Biotechnol J 2024;23:3327–3341. doi:10.1016/j.csbj.2024.09.001, PMID:39310281.

[15] Sui M, Feng S, Liu G, Chen B, Li Z, Shao P. Deep eutectic solvent on extraction of flavonoid glycosides from Dendrobium officinale and rapid identification with UPLC-triple-TOF/MS. Food Chem 2023;401:134054. doi:10.1016/j.foodchem.2022.134054, PMID:36103742.

[16] Zhao TT, Zhang Y, Zhang CQ, Chang YF, Cui MR, Sun Y, *et al*. Combined with UPLC-Triple-TOF/MS-based plasma lipidomics and molecular pharmacology reveals the mechanisms of schisandrin against Alzheimer's disease. Chin Med 2023;18(1):11. doi:10.1186/s13020-023-00714-y, PMID:36747236.

[17] Chen LH, Zhang YB, Yang XW, Xu W, Wang YP. Characterization and quantification of ginsenosides from the root of Panax quinquefolius L. by integrating untargeted metabolites and targeted analysis using UPLC-Triple TOF-MS coupled with UFLC-ESI-MS/MS. Food Chem 2022;384:132466. doi:10.1016/j.foodchem.2022.132466, PMID:35202989.

[18] Li H, Song Y, Zhang H, Wang X, Cong P, Xu J, *et al*. Comparative lipid profile of four edible shellfishes by UPLC-Triple TOF-MS/MS. Food Chem 2020;310:125947. doi:10.1016/j.foodchem.2019.125947, PMID:31841939.

[19] Jia W, Bi Q, Jiang S, Tao J, Liu L, Yue H, *et al*. Hypoglycemic activity of Codonopsis pilosula (Franch.) Nannf. in vitro and in vivo and its chemical composition identification by UPLC-Triple-TOF-MS/MS. Food Funct 2022;13(5):2456–2464. doi:10.1039/d1fo03761g, PMID:35147627.

[20] Liang C, Yao Y, Ding H, Li X, Li Y, Cai T. Rapid classification and identification of chemical components of Astragali radix by UPLC-Q-TOF-MS. Phytochem Anal 2022;33(6):943–960. doi:10.1002/pca.3150, PMID:35726352.

[21] Liu X, Liu J, Fu B, Chen R, Jiang J, Chen H, *et al*. DCABM-TCM: A Database of Constituents Absorbed into the Blood and Metabolites of Traditional Chinese Medicine. J Chem Inf Model 2023;63(15):4948–4959. doi:10.1021/acs.jcim.3c00365, PMID:37486750.

[22] Chau SL, Huang ZB, Song YG, Yue RQ, Ho A, Lin CZ, *et al*. Comprehensive Quantitative Analysis of SQ Injection Using Multiple Chromatographic Technologies. Molecules 2016;21(8):1092. doi:10.3390/molecules21081092, PMID:27548134.

[23] Xu W, Zhou F, Zhu Q, Bai M, Luo T, Zhou L, *et al*. Calycosin-7-O-β-D-glucoside attenuates palmitate-induced lipid accumulation in hepatocytes through AMPK activation. Eur J Pharmacol 2022;925:174988. doi:10.1016/j.ejphar.2022.174988, PMID:35490724.

[24] Su J, Gao C, Xie L, Fan Y, Shen Y, Huang Q, *et al*. Astragaloside II Ameliorated Podocyte Injury and Mitochondrial Dysfunction in Streptozotocin-Induced Diabetic Rats. Front Pharmacol 2021;12:638422. doi:10.3389/fphar.2021.638422, PMID:33796024.

[25] Chen Z, Su Y, Ding J, He J, Lai L, Song Y. Lobetyolin protects mice against LPS-induced sepsis by downregulating the production of inflammatory cytokines in macrophage. Front Pharmacol 2024;15:1405163. doi:10.3389/fphar.2024.1405163, PMID:38799158.

[26] Sevimli-Gür C, Onbaşılar I, Atilla P, Genç R, Cakar N, Deliloğlu-Gürhan I, *et al*. In vitro growth stimulatory and in vivo wound healing studies on cycloartane-type saponins of Astragalus genus. J Ethnopharmacol 2011;134(3):844–850. doi:10.1016/j.jep.2011.01.030, PMID:21291980.

[27] Ziyang T, Xirong H, Chongming A, Tingxin L. The potential molecular pathways of Astragaloside-IV in colorectal cancer: A systematic review. Biomed Pharmacother 2023;167:115625. doi:10.1016/j.biopha.2023.115625, PMID:37793276.

[28] Xu F, Cui WQ, Wei Y, Cui J, Qiu J, Hu LL, *et al*. Astragaloside IV inhibits lung cancer progression and metastasis by modulating macrophage polarization through AMPK signaling. J Exp Clin Cancer Res 2018;37(1):207. doi:10.1186/s13046-018-0878-0, PMID:30157903.

[29] Jiang K, Lu Q, Li Q, Ji Y, Chen W, Xue X. Astragaloside IV inhibits breast cancer cell invasion by suppressing Vav3 mediated Rac1/MAPK signaling. Int Immunopharmacol 2017;42:195–202. doi:10.1016/j.intimp.2016.10.001, PMID:27930970.

[30] Fang Gong Y, Hou S, Xu JC, Chen Y, Zhu LL, Xu YY, *et al*. Amelioratory effects of astragaloside IV on hepatocarcinogenesis via Nrf2-mediated pSmad3C/3L transformation. Phytomedicine 2023;117:154903. doi:10.1016/j.phymed.2023.154903, PMID:37301185.

[31] Wang Y, Zhang Z, Cheng Z, Xie W, Qin H, Sheng J. Astragaloside in cancer chemoprevention and therapy. Chin Med J (Engl) 2023;136(10):1144–1154. doi:10.1097/CM9.0000000000002661, PMID:37075760.

[32] Yang C, Wu C, Xu D, Wang M, Xia Q. AstragalosideII inhibits autophagic flux and enhance chemosensitivity of cisplatin in human cancer cells. Biomed Pharmacother 2016;81:166–175. doi:10.1016/j.biopha.2016.03.025, PMID:27261591.

[33] He W, Tao W, Zhang F, Jie Q, He Y, Zhu W, *et al*. Lobetyolin induces apoptosis of colon cancer cells by inhibiting glutamine metabolism. J Cell Mol Med 2020;24(6):3359–3369. doi:10.1111/jcmm.15009, PMID:31990147.
[34] Rutter BD, Innes RW. Extracellular Vesicles in Phytopathogenic Fungi. Extracell Vesicles Circ Nucleic Acids 2023;4(1):90–106. doi:10.20517/evcna.2023.04.
[35] Mu N, Li J, Zeng L, You J, Li R, Qin A, *et al*. Plant-Derived Exosome-Like Nanovesicles: Current Progress and Prospects. Int J Nanomedicine 2023;18:4987–5009. doi:10.2147/IJN.S420748, PMID:37693885.
[36] Liu H, Geng Z, Su J. Engineered mammalian and bacterial extracellular vesicles as promising nanocarriers for targeted therapy. Extracell Vesicles Circ Nucleic Acids 2022;3(1):63–86. doi:10.20517/evcna.2022.04.
[37] Zhao B, Lin H, Jiang X, Li W, Gao Y, Li M, *et al*. Exosome-like nanoparticles derived from fruits, vegetables, and herbs: innovative strategies of therapeutic and drug delivery. Theranostics 2024;14(12):4598–4621. doi:10.7150/thno.97096, PMID:39239509.
[38] Cai Q, Halilovic L, Shi T, Chen A, He B, Wu H, *et al*. Extracellular vesicles: cross-organismal RNA trafficking in plants, microbes, and mammalian cells. Extracell Vesicles Circ Nucl Acids 2023;4(2):262–282. doi:10.20517/evcna.2023.10, PMID:37575974.
[39] Simbari F, McCaskill J, Coakley G, Millar M, Maizels RM, Fabriás G, *et al*. Plasmalogen enrichment in exosomes secreted by a nematode parasite versus those derived from its mouse host: implications for exosome stability and biology. J Extracell Vesicles 2016;5:30741. doi:10.3402/jev.v5.30741, PMID:27389011.
[40] Rigalli JP, Gagliardi A, Diester K, Bajraktari-Sylejmani G, Blank A, Burhenne J, *et al*. Extracellular Vesicles as Surrogates for the Regulation of the Drug Transporters ABCC2 (MRP2) and ABCG2 (BCRP). Int J Mol Sci 2024;25(7):4118. doi:10.3390/ijms25074118, PMID:38612927.
[41] Chen LH, Zhang YB, Yang XW, Xu J, Wang ZJ, Sun YZ, *et al*. Application of UPLC-Triple TOF-MS/MS metabolomics strategy to reveal the dynamic changes of triterpenoid saponins during the decocting process of Asian ginseng and American ginseng. Food Chem 2023;424:136425. doi:10.1016/j.foodchem.2023.136425, PMID:37263091.
[42] Guo W, Xu X, Xiao Y, Zhang J, Shen P, Lu X, *et al*. Salvianolic acid C attenuates cerebral ischemic injury through inhibiting neuroinflammation via the TLR4-TREM1-NF-κB pathway. Chin Med 2024;19(1):46. doi:10.1186/s13020-024-00914-0, PMID:38468280.
[43] Shi L, Deng J, He J, Zhu F, Jin Y, Zhang X, *et al*. Integrative transcriptomics and proteomics analysis reveal the protection of Astragaloside IV against myocardial fibrosis by regulating senescence. Eur J Pharmacol 2024;975:176632. doi:10.1016/j.ejphar.2024.176632, PMID:38718959.
[44] Li X, Mu Y, Hua M, Wang J, Zhang X. Integrated phenotypic, transcriptomics and metabolomics: growth status and metabolite accumulation pattern of medicinal materials at different harvest periods of Astragalus Membranaceus Mongholicus. BMC Plant Biol 2024;24(1):358. doi:10.1186/s12870-024-05030-7, PMID:38698337.
[45] Zhang J, Zhong D, Hou F, Xie X, Gao J, Peng C. Transcriptomics-based Study on the Mechanism of Heart Failure Amelioration by Water Decoction and Water-soluble Alkaloids of Fuzi. Future Integr Med 2024;3(2):75–86. doi:10.14218/fim.2024.00005.